

SEISMIC ASSESSMENT OF SUSPENDED CEILING THROUGH DYNAMIC NONLINEAR ANALYSES

Alessandro PALMERI¹, Thomas ARMITAGE², Mariateresa LOMBARDO³,
Laura FIORIN⁴ & Matthew HARRISON⁵

Abstract: *The detrimental effects of irregularities in plan and elevation on the seismic performance of building structures are well documented in the literature. Conversely, researchers and practitioners have paid little attention to the effects of structural irregularities on the seismic response of non-structural components (NSCs). This aspect deserves more detailed investigations, as the poor seismic behaviour of NSCs can put people's life at risk and cause significant direct and indirect economic losses. Unsurprisingly then, current design methods do not demonstrate the seismic safety of NSCs have many shortcomings. In this paper, nonlinear dynamic analyses are used to rigorously quantify the seismic performance of suspended metal ceilings, a particularly important type of NSCs due to their diffuse presence in both public and private buildings. The analyses are carried out within the PEER's framework of performance-based earthquake engineering. Nonlinear time-history analyses are executed on a case-study building for increasing levels of the seismic intensity measure and varying degrees of structural irregularity in plan and in elevation, while linear elastic and nonlinear constant-ductility floor spectra allow evaluating the seismic demand on the suspend ceilings, whose mechanical parameters have been calibrated against the results of an extensive experimental campaign.*

Introduction

Suspended ceilings are light ceiling systems normally utilised in commercial or office buildings. They typically consist of ceiling tiles supported by a metal grid, which in turn is suspended from the load-bearing floor through metal wires or ties. The void created underneath the floors of the building can be used for wiring, piping, light fixtures and HVAC (heating, ventilation, and air-conditioning) systems.

During earthquakes, different failure mechanisms can occur in the metal ceilings, including dislodging of panels, fall of panels, perimeter failure, connection failure, pounding with other building components, etcetera (e.g. Dhakal *et al*, 2011; Dhakal and MacRae, 2013). These mechanisms can result in injuries and even deaths, seldomly; more frequently, they affect the functionality of the building in the aftermath of a seismic event, which is particularly worrying in the case of hospitals and other facilities key to civil protection; furthermore, the cost for repairing or replacing damaged metal ceilings can be significant.

In earthquake engineering, suspended ceilings are an important example of non-structural components (NSCs), whose performance should be properly accounted for when quantifying the expected losses due to a certain seismic event (e.g. NIST GCR 17-917-44). Approximate expressions are available in design codes to estimate the seismic forces on NSCs, e.g. ASCE 7-16 and BS EN 1998-1, but several shortcomings affects their application in the context of a proper performance-based design (see e.g. Filiatrault and Sullivan, 2014; Filiatrault *et al*, 2018), including: *i*) the empirical assumption that the peak floor acceleration increases linearly along the height of the building, thus neglecting the effects of higher modes of vibration on the seismic response of the building; *ii*) the characteristics of the nonlinear response of both the supporting

¹ Reader in Structural Engineering & Dynamics, Loughborough University, Loughborough, UK, A.Palmeri@Lboro.ac.uk and Dynamics.Structures@gmail.com

² MEng finalist, Loughborough University, Loughborough, UK

³ Senior Lecturer in Structural Engineering & Design, Loughborough University, Loughborough, UK

⁴ KTP Associate, Loughborough University and SAS International, Loughborough and Reading, UK

⁵ Head of Technical, SAS International, Reading, UK

42 structure and NSC are not accounted for; *iii*) the adoption of a force reduction factor (i.e. the
43 behaviour factor q_a in BS EN 1998-1) to NSCs is difficult to justify and potentially misleading.

44 A rigorous approach to the seismic analysis and design of NSCs would require the numerical
45 integration of the nonlinear equations of motion for both the primary (load-bearing) structure and
46 the NSCs. As suspended ceilings are relatively light in comparison to the floors which they are
47 attached to, their feedback force on the primary structure can be neglected (see e.g. Chen and
48 Soong, 1988; Villaverde, 1997; Singh *et al.*, 2006a and 2006b; Muscolino and Palmeri, 2007;
49 Kasinos *et al.*, 2015). In this “cascade approach”, the seismic response of primary structure and
50 secondary system are computed in sequence: that is, first the primary structure, neglecting the
51 presence of any NSC; then the secondary system, which is excited by the absolute motion of the
52 primary structure at the contact points with the secondary system. If the latter can be modelled
53 as a SDoF (single degree of freedom) oscillator singly connected to the primary structure, the
54 cascade approach becomes equivalent to the application of the so-called floor spectra, i.e.
55 response spectra in which the seismic input is the absolute acceleration at a given contact point
56 in the primary structure.

57 It is well known that irregularities in a building structure can severely affected its modes of
58 vibration and, ultimately, its seismic response (e.g. Shahrooz and Moehle, 1990; Wood, 1992;
59 Valmundsson EV and Nau JM, 1997; De Stefano and Pintucchi, 2008; Anagnostopoulos *et al.*,
60 2015). Architectural and functional requirements, as well as accidental variations, are all potential
61 sources of irregularity, either in plan (i.e. asymmetric distributions of mass, stiffness and strength)
62 or in elevation (e.g. due to discontinuities in structural elements or variations in occupancy), which
63 can result in large torsional effects of deformations concentrated in certain soft storeys.

64 Comparatively, less attention has been paid to the effects that irregularities in the primary
65 structure can have on the seismic performance of NSCs. Aldeka and his co-authors (Aldeka *et al.*,
66 2014; Aldeka *et al.*, 2015) have shown that Eurocode 8 predictions (BS EN 1998-1) tend to
67 underestimate the seismic response of NSCs mounted on the flexible sides of RC (reinforced
68 concrete) MRFs (moment resisting frames) with irregularities in plan. Kasinos *et al.* (2015) have
69 investigated the seismic response of secondary MDoF (multiple degrees of freedom) systems
70 multi-connected to primary multi-storey MRFs with various degrees of irregularity; the results of
71 their parametric study show that the effects of irregularities in the primary structure tend to affect
72 more acceleration-sensitive NSCs (such as suspended ceilings) than drift-sensitive NSCs. More
73 recently, Surana *et al.* (2018) have proposed some new spectral amplification functions for the
74 seismic design of acceleration-sensitive NSCs in hill-side buildings, affected by a combination of
75 irregularities in plan and elevation.

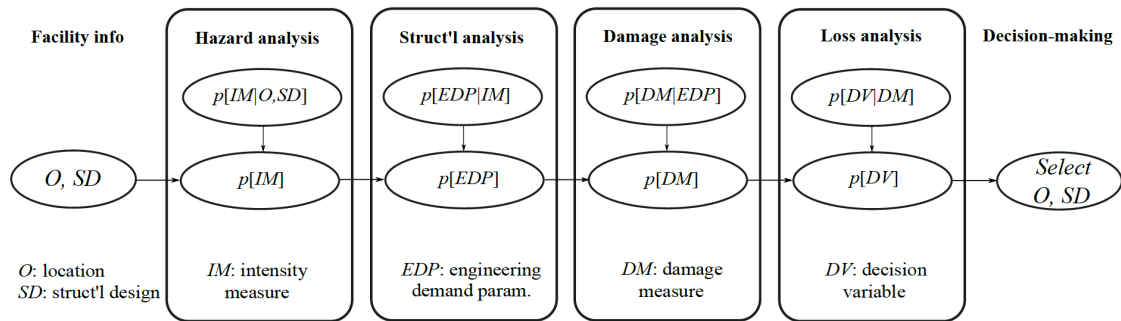
76 In this paper, the preliminary results of an extensive parametric study are presented, aimed at
77 quantifying in a rigorous manner the effects that irregularities in the load-bearing structure can
78 have on the seismic response of metal ceilings installed at different locations in a multi-storey
79 case-study building. The analysis of the results supports the claim that simplified design
80 expressions for NSCs, such as those provided by ASCE 7-16 and BS EN 1998-1, do not provide
81 reliable indications on the actual performance of these elements. Instead, seismic damage
82 occurring in metal ceilings can be better analysed through a probabilistic characterisation of a
83 relevant EDP (engineering demand parameter). The latter has been taken in this study as the
84 ordinate of the floor spectrum in terms of pseudo-accelerations for the fundamental period of
85 vibration of the metal ceiling, calculated for increasing values of the IM (intensity measure) of the
86 seismic input and at the locations of interest in the building.

87 **Methods**

88 *Performance-based earthquake engineering (PBEE)*

89 Performance-based engineering (PBE) is a general methodology that enables the rigorous
90 probabilistic assessment of the performance of structural systems and infrastructural facilities
91 when subject to natural and man-made hazards (Barbato *et al.*, 2014). One of the main reasons
92 underpinning the engineers' quest to overcome prescriptive seismic design codes is that,
93 although they generally provide adequate protection against the no-collapse requirement (NCR),
94 direct and indirect economic losses caused by seismic events of relatively low-to-moderate
95 intensity proved historically to be excessively high (e.g. Ghobarah, 2001; de Luca di Roseto *et al.*,
96 2018), particularly because of damage occurred to NSCs. The most popular framework of
97 performance-based earthquake engineering (PBEE) is by far the formulation developed by the

98 PEER (Pacific Earthquake Engineering Research) centre since the early 2000s (Porter, 2003),
 99 which consists of four successive stages, namely: 1) hazard analysis, 2) structural analysis, 3)
 100 damage analysis and 4) loss analysis (see Figure 1).



101
 102 *Figure 1. PBEE framework, as conceived by the PEER centre (adapted from Moehle and*
 103 *Deierlein, 2004).*

104 The PEER's framework can be also expressed mathematically through the following triple integral
 105 (Lee and Mosalam, 2006):

106
$$p[DV|\{O,SD\}] = \int \int \int p[DV|DM] p[DM|EDP] p[EDP|IM] p[IM|\{O,SD\}] dIM dEDP dDM, \quad (1)$$

107 where the symbols $p[X]$ and $p[X|Y]$ are to the probability density function (PDF) of X and the
 108 conditional PDF (CPDF) of X given Y; IM, EDP, DM and DV are the relevant intensity
 109 measure, engineering demand parameter, damage measure and decision variable in the design
 110 problem; while O and SD are the set of parameters characterising location and structural
 111 design. In this paper, only the first two stage of the PBEE will be considered, leading to the
 112 probabilistic characterisation of IM and EDP, as detailed in the following subsections.

113 *Case-study structure*

114 A 3-by-2-bay 5-storey steel MRF adapted from the work by Araújo and Castro (2017) has been
 115 used as case-study structure. The inter-storey height is 3.50 m, with the only exception of the
 116 ground level, whose height is 4.50 m, for an overall building height of 18.5 m; all the bays are
 117 6x6 m, for an overall plan area of 216 m², doubly symmetrical in its original configuration. Dead
 118 load of 4.0 kN/m² and live load of 3.0 kN/m² have been assumed. Columns' cross sections are
 119 HE 450B for the ground level, HE 400 B for the intermediate levels and HE 300 B for the top two
 120 levels; beams' cross sections are IPE 330 for the bottom two storeys and IPE 300 for the other
 121 ones; the structural steel grade was specified as S275. The first three modal period of vibration
 122 were $T_1 = 0.46$ s in the transverse direction, $T_2 = 0.38$ s for the first torsional mode and $T_3 = 0.33$ s
 123 in the longitudinal direction.

124 In the following, the frame detailed above will be referred to as layout L0 (see Figure 2(a)), without
 125 any irregularity. Layouts L1 to L5 have also been considered, with different levels of irregularity,
 126 namely:

- 127 • L1, characterised by an irregularity in elevation due to the suppression of 2 bays in each of
 128 the top two levels (see Figure 2(b));
- 129 • L2, with increased irregularity in elevation, the suppression of 2 bays in each of the top four
 130 levels (see Figure 2(c));
- 131 • L3, with an irregularity in plan, due to enlarged cross sections for the columns located on
 132 one of the long sides of the building (resulting in an eccentricity between centre of mass
 133 and centre of rigidity of about 1.0 m, see Figure 2(d));
- 134 • L4, with an increased irregularity in plan, due to a further enlargement of column's cross
 135 sections (with the eccentricity increased to about 1.5 m, see Figure 2(d));
- 136 • L5, a combination of irregularities in plan and elevation (namely L2 and L4, see Figure 2(e)).

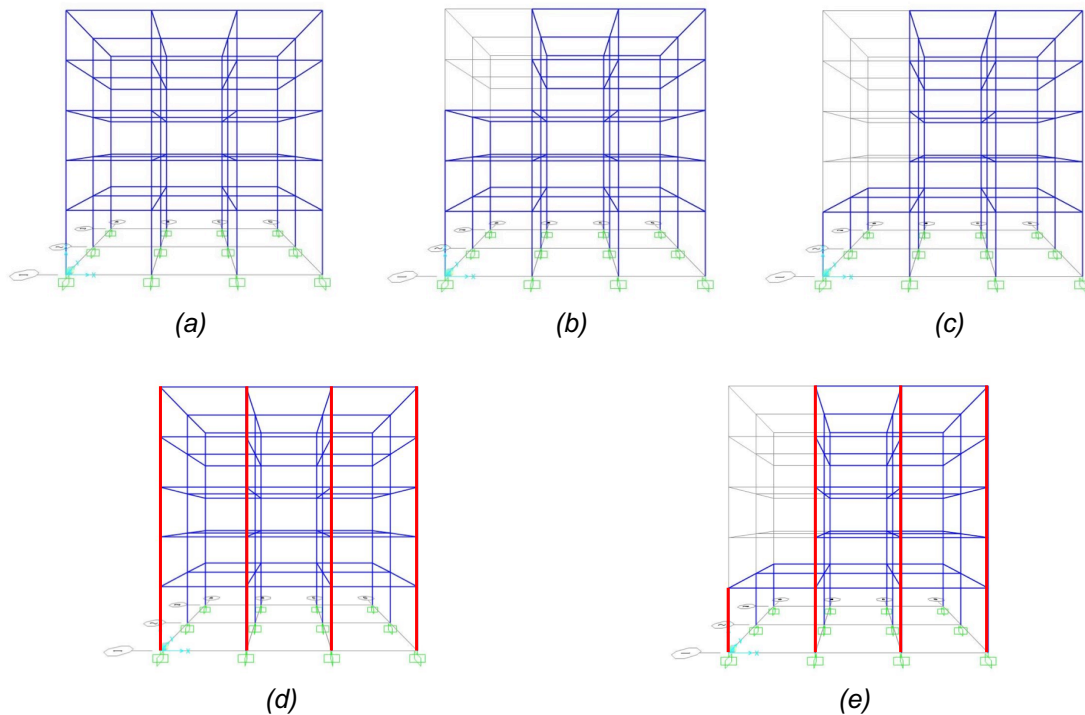


Figure 2. Various structural layouts considered as part of the parametric study.

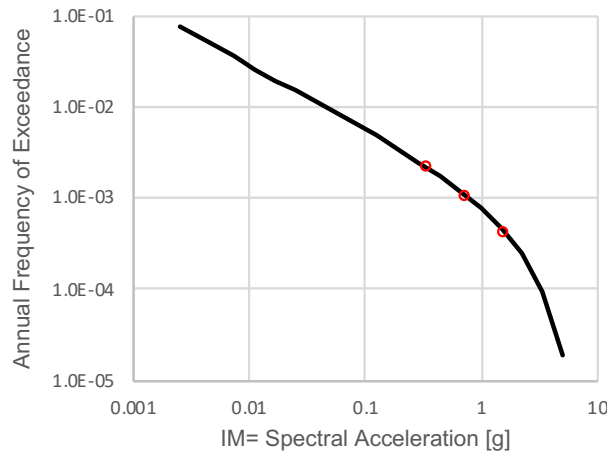
137

138 *Hazard analysis*

139 The frame by Araújo and Castro (2017) was designed for a location in Lisbon, Portugal. The PGA
 140 (peak ground acceleration) for this original site is approximately 0.2 g for a seismic event with
 141 PoE (probability of exceedance) of 10% in 50 years (corresponding to a return period $T_R = 475$ yr,
 142 i.e. the NCR). A site with the same PGA for the NCR has been identified in the USA, near
 143 Charleston, South Carolina (latitude= 33.212° N, longitude= 79.980° W).

144

145 For this new design site, the Unified Hazard Tool (UHT) developed by the NSHMP (National
 146 Seismic Hazard Mapping Project) within the Earthquake Hazards Program (EHP) of the USGS
 147 (US Geological Survey) has been used, assuming: site class “B/C boundary”, corresponding to
 148 an average shear velocity in the upper 30m of $V_S^{(30)} = 760$ m/s; spectral period $\bar{T} = 0.20$ s, which
 149 was the value closest to the fundamental period of vibration T_1 among the available options;
 150 earthquake hazard model “Dynamic: Conterminous US 2014 (v4.1.1)” (Earthquake.USGS.gov,
 151 2019). $N_{IM} = 3$ return periods have been considered, namely $T_R = 475$, 975 and 2475 yr (or,
 152 equivalently, $N_{IM} = 3$ annual frequencies of exceedance, i.e. $\lambda_{IM} = T_R^{-1} = 0.00211$, 0.00103 and
 153 0.00040), for which the IM takes the values $S_{pa}(\bar{T}) = 0.344$, 0.750 and 1.612g. The hazard
 154 curve for the site under consideration is plotted within Figure 3, where the red circles indicate the
 155 chosen levels of the IM.



156
157

Figure 3. Hazard curve for the sire under investigation in South Coraline.

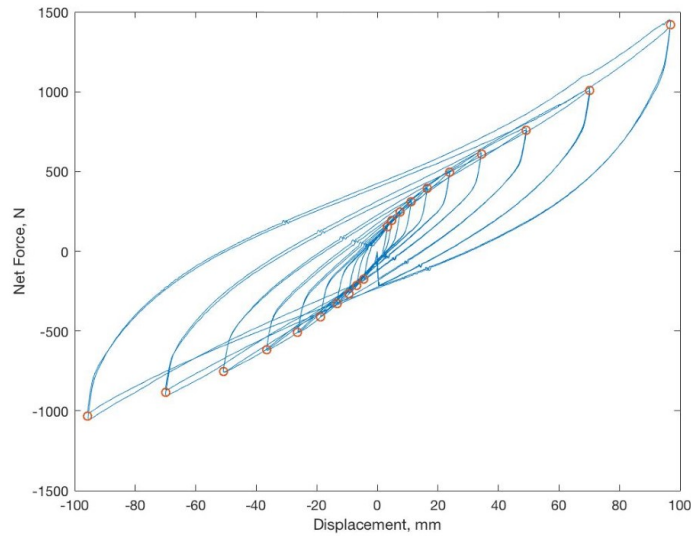
158 The disaggregation of the seismic hazard has been performed with the UHT, returning mean
159 magnitude $M_w = 6.5$ to 7.1 and mean rupture distance $r_{Rup} = 23$ to 13km when increasing the
160 IM. For each value of the IM, a suite of $N_{EQ} = 120$ earthquake records have been found in the
161 PEER’s ground motion database (NGAwest2.Berkeley.edu, 2019), divided in four quadrants
162 $\{M_w, r_{Rup}\}$, depending on whether they are characterised by magnitude and rupture distance
163 smaller or larger than the corresponding mean values. Each accelerogram has then been scaled
164 to match the value of the IM.

165 *Structural analysis*

166 Each of the $N_{SD} = 6$ variants of the case-study frame (i.e. layouts L0 to L5) was analysed with
167 the commercial structural analysis program SAP2000 (CSiamerica.com, 2019). Standard plastic
168 hinges were defined at the ends of the steel beams (simple flexure “ M_3 ”) and columns (axial-
169 flexure interaction “ $P-M_2-M_3$ ”), according to FEMA-356 (2000), and Rayleigh’s damping has been
170 assumed for the load-bearing frame, with an equivalent viscous damping ratio of 5% at $T = 0.1$
171 and 1.0s . The gravitational actions were initially applied to each frame (100% of the dead load
172 and 30% of the live load) through a nonlinear static case, before the N_{EQ} ground accelerations
173 could be applied. The nonlinear time-history analyses have been performed with the classical
174 Hilber-Hughes-Taylor integration scheme (Hilber *et al*, 1977). Overall, $N_{sym} = N_{SD} \times N_{IM} \times N_{EQ} =$
175 2160 nonlinear time-history analyses have been carried out.

176 *Nonlinear floor spectra*

177 For each simulation performed with SAP2000, the time history of the absolute acceleration in
178 various control points on the frame have been recorded, including the corner nodes at the top
179 storey. According to the cascade approach discussed in the Introduction, the latter have been
180 used as base motion exciting a series of nonlinear SDoF oscillators, conveniently calibrated
181 against the data collected through an extensive experimental campaign conducted on full-scale
182 metal ceilings with different configurations and technologies (preliminary results have been
183 presented in the work by Fiorin *et al* (2019)). Figure 4 shows an example of hysteretic loops
184 obtained through quasi-static cyclic testing.



185

186

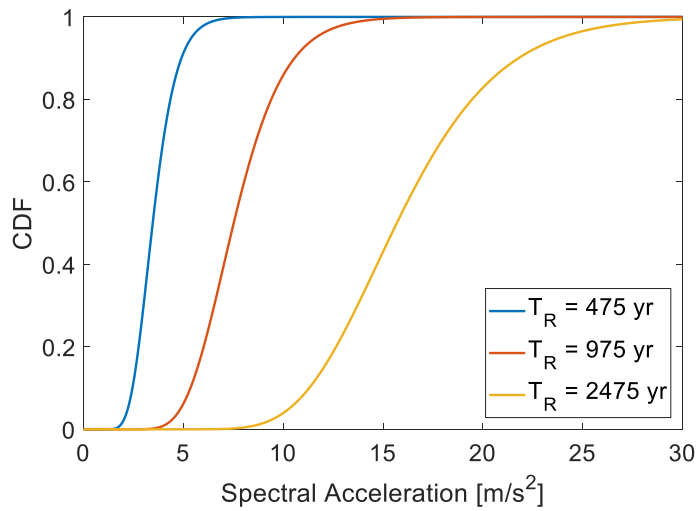
Figure 4. Typical hysteretic loops of metal ceilings obtained through quasi-static cyclic tests.

187

Results and Discussion

188

For the sake of conciseness, only selected results are presented in what follows.



189

190

191

Figure 5. Probability distribution for the EDP chosen to characterise the performance of the metal ceiling.

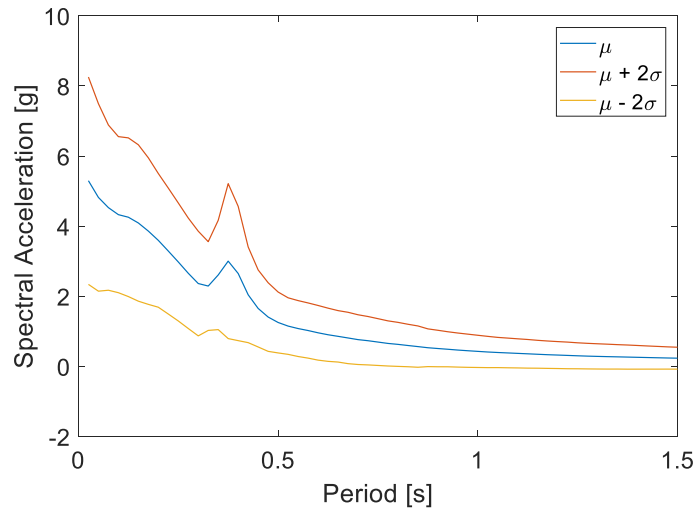
192

193

194

195

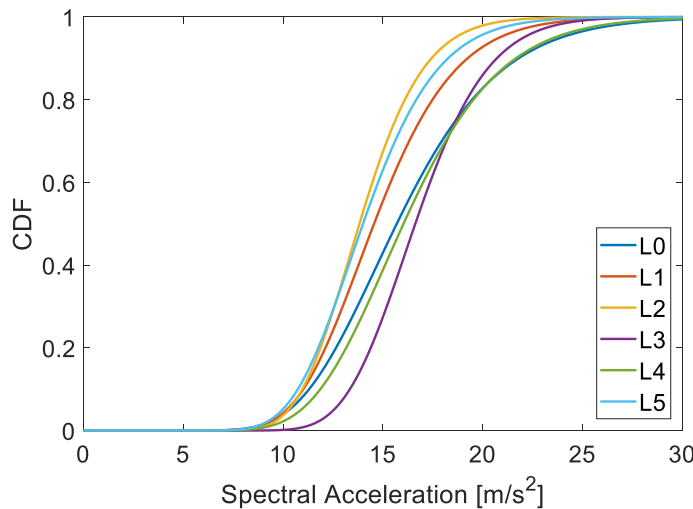
Figure 5 shows the CDF (cumulative distribution function) of the EDP taken as the spectral acceleration of the metal ceiling installed in the frame of layout L0, for the three value of the IM. As expected, the higher the IM, the higher the EDP. Due to the combined nonlinearity of structural frame and metal ceiling, the EPDs are not directly proportional to the value of IM.



196
197

Figure 6. Variability in the nonlinear floor spectra.

198 Figure 6 shows the aleatory variability affecting the nonlinear floor spectra, assuming that the
 199 ductility of the secondary oscillator is $\mu_s = 6$ and its period of vibration T_s varies between 0.025
 200 and 1.50s. The plots of Figure 6 have been obtained for the lowest value of the intensity measure,
 201 namely for $T_R = 475$ yr, and layout L0. It is evident the dynamic amplification occurring when the
 202 metal ceiling is in tune with the fundamental mode of vibration of the primary structure (in this
 203 case, $T_s = T_2$).



204
205

Figure 7. Probability distribution for the EDP for different structural irregularities.

206 Finally, Figure 7 presents a comparison of the CDFs of the EPD calculated for the six different
 207 structural layouts, from L0 (regular frame) to L5 (combined irregularities in plan and in elevation).
 208 Although no clear trend can be observed from this figure, it is evident the impact that irregularities
 209 can have on acceleration-sensitive NSCs, and in particular metal ceilings. For instance, the
 210 variability on the median (CDF= 0.50) can be as large as 20%.

211 **Conclusions**

212 In this paper, the results of an extensive simulation campaign have been presented, aimed at
 213 quantifying the effects of irregularities in the load-bearing structure on the seismic performance
 214 of suspended metal ceilings. While no definite trends have been identified, the case-study
 215 structure has clearly shown the importance to account for the presence of structural irregularities
 216 when analysing non-structural components (NSCs), with variations in the order of 20%. A similar
 217 level of variability has been observed for the aleatory nature of the seismic action.

218 The numerical results confirm the inadequacy of force-based design provisions for NSCs in
 219 current design codes, which do not consider the impact of soft storeys, eccentricities in plan and
 220 other forms of structural irregularity. Further investigations are needed to establish clear
 221 correlations between structural irregularities and the seismic performance of NSCs, which in turn
 222 can guide designer and specifiers.

223 References

- 224 Aldeka AB, Chan AHC and Dirar S (2014), Response of non-structural components mounted on
 225 irregular RC buildings: Comparison between FE and EC8 predictions, *Earthquake and*
 226 *Structures*, 6(4): 351-373.
- 227 Aldeka AB, Dirar S, Chan AHC and Martinez-Vazquez P (2015), Seismic response of non-
 228 structural components attached to reinforced concrete structures with different eccentricity
 229 ratios, *Earthquake and Structures*, 8(5): 1069-1089.
- 230 Anagnostopoulos SA, Kyrkos MT and Stathopoulos KG (2015), Earthquake induced torsion in
 231 buildings: Critical review and state of the art, *Earthquake and Structures*, 8(2), pp. 305-377.
- 232 Araújo M and Castro JM (2017), Simplified procedure for the estimation of local inelastic
 233 deformation demands for seismic performance assessment of buildings, *Earthquake*
 234 *Engineering and Structural Dynamics*, 46(3): 491-514.
- 235 Barbato M, Palmeri A and Petrini F (2014), Special issue on performance-based engineering,
 236 *Engineering Structures*, 78: 1-2.
- 237 ASCE 7-16:2016, *Minimum Design Loads for Buildings and Other Structures*, American Society
 238 of Civil Engineers, Reston, Virginia.
- 239 BS EN 1998-1:2004+A1:2013: *Eurocode 8 – Design Provisions for Earthquake Resistant*
 240 *Structures*, Comité Européen de Normalisation, Brussels, Belgium.
- 241 Chen Y and Soong TT (1988), Seismic response of secondary systems, *Engineering*
 242 *Structures*, 10(4): 218-228.
- 243 CSiamerica.com (2019), *Structural Software for Analysis and Design, SAP2000* [online],
 244 Available at: <https://www.csiamerica.com/products/sap2000> [Accessed: 24 April 2019].
- 245 de Luca di Roseto A, Palmeri A and Gibb AG (2018), Performance-based seismic design of
 246 steel structures accounting for fuzziness in their joint flexibility, *Soil Dynamics and*
 247 *Earthquake Engineering*, 115: 799-814.
- 248 De Stefano M and Pintucchi B (2008), A review of research on seismic behaviour of irregular
 249 building structures since 2002, *Bulletin of Earthquake Engineering*, 6(2): 285-308.
- 250 Dhakal RP, MacRae GA and Hogg K (2011), Performance of ceilings in the February 2011
 251 Christchurch earthquake, *Bulletin of the New Zealand Society for Earthquake Engineering*,
 252 44(4): 379-389.
- 253 Dhakal RP, MacRae GA (2013), Ceiling systems design and installation lessons from the
 254 Canterbury Earthquakes, *10th International Conference on Urban Earthquake Engineering*,
 255 Tokyo, Japan.
- 256 Earthquake.USGS.gov (2019), *Unified Hazard Tool* [online], Available at:
 257 <https://earthquake.usgs.gov/hazards/interactive/index.php> [Accessed: 24 April 2019].
- 258 FEMA-356 (2000), *Prestandard and Commentary for Seismic Rehabilitation of Buildings*,
 259 Federal Emergency Management Agency, Washington DC.
- 260 Filiatrault A, Perrone D, Merino RJ and Calvi GM (2018), Performance-based seismic design of
 261 nonstructural building elements, *Journal of Earthquake Engineering*, g, DOI:
 262 10.1080/13632469.2018.1512910.
- 263 Filiatrault A and Sullivan T (2014), Performance-based seismic design of nonstructural building
 264 components: The next frontier of earthquake engineering, *Earthquake Engineering and*
 265 *Engineering Vibration*, 13(1): 17-46.
- 266 Fiorin L, Palmeri A, Lombardo M and Harrison (2019), Innovative experimental methodology to
 267 evaluate the seismic performance of suspended ceilings, *4th International Workshop on the*
 268 *Seismic Performance of Non-Structural Elements*, Pavia, Italy.
- 269 Ghobarah A (2001), Performance-based design in earthquake engineering: state of
 270 development, *Engineering Structures*, 23(8): 878-884.

- 271 Hilber HM, Hughes TJR, Taylor RL (1977), Improved numerical dissipation for time integration
272 algorithms in structural dynamics, *Earthquake Engineering and Structural Dynamics*, 5(3):
273 283-292.
- 274 Kasinos S, Palmeri A and Lombardo M (2015), Seismic response of subsystems in irregular
275 buildings, *12th International Conference on Applications of Statistics and Probability in Civil
276 Engineering*, Vancouver, Canada, DOI:n 10.14288/1.0076300.
- 277 Kasinos S, Palmeri A and Lombardo M (2016), Performance-based seismic analysis of light
278 SDoF secondary substructures, *Proceedings of the Institution of Civil Engineers: Structures
279 and Buildings*, 169(8): 643-654.
- 280 Lee TH and Mosalam KM (2006), *Probabilistic Seismic Evaluation of Reinforced Concrete
281 Structural Components and Systems*, PEER Report 2006/04, University of California,
282 Berkeley, California.
- 283 Moehle JP and Deierlein GG (2004), A framework methodology for performance-based
284 earthquake engineering, *13th World Conference on Earthquake Engineering*, Vancouver,
285 Canada, Paper No 679.
- 286 Muscolino G and Palmeri A (2007), An earthquake response spectrum method for linear light
287 secondary substructures, *ISET Journal of Earthquake Technology*, 44(1): 193-211.
- 288 NGAwest2.Berkeley.edu (2019), *PEER Ground Motion Database* [online], Available at:
289 <https://ngawest2.berkeley.edu/site> [Accessed: 24 April 2019].
- 290 NIST GCR 17-917-44:2017, *Seismic Analysis, Design, and Installation of Nonstructural
291 Components and Systems – Background and Recommendations for Future Work*, Applied
292 Technology Council, Redwood City, California, DOI: 10.6028/NIST.GCR.17-917-44.
- 293 Porter KA (2003), An overview of PEER's performance-based earthquake engineering
294 methodology, *9th International Conference on Applications of Statistics and Probability in
295 Civil Engineering*, San Francisco, California.
- 296 Shahrooz BM and Moehle JP (1990), Seismic response and design of setback buildings.
297 *Journal of Structural Engineering*, 116(5): 1423-1439.
- 298 Singh MP, Moreschi LM, Suárez LE and Matheu EE (2006a), Seismic design forces. I: Rigid
299 nonstructural components, *Journal of Structural Engineering*, 132(10): 1524-1532.
- 300 Singh MP, Moreschi LM, Suárez LE and Matheu EE (2006b), Seismic design forces. II: Flexible
301 nonstructural components, *Journal of Structural Engineering*, 132(10): 1533-1542.
- 302 Surana M, Singh Y and Lang DH (2018), Effect of irregular structural configuration on floor
303 acceleration demand in hill-side buildings, *Earthquake Engineering and Structural
304 Dynamics*, 47(10): 2032-2054.
- 305 Valmundsson EV and Nau JM (1997), Seismic response of building frames with vertical
306 structural irregularities, *Journal of Structural Engineering*, 123(1): 30-40.
- 307 Villaverde R (1997), Seismic design of secondary structures: State of the art, *Journal of
308 Structural Engineering*, 123(8): 1011-1019.
- 309 Wood SL (1992), Seismic response of R/C frames with irregular profiles. *Journal of Structural
310 Engineering*, 118(2): 545-566.